Chemically reacting transverse plume

P. Ranjan,[*] K. Perez, T. Alvarado, B. Potter,[†] and R. E. Breidenthal[‡]
William E. Boeing Department of Aeronautics and Astronautics, University of Washington, Seattle, Washington 98195-2180, USA

(Received 14 October 2014; accepted 30 June 2020; published 14 September 2020)

The flame length of a plume in incompressible cross-flow is analyzed and the results are compared with those obtained in a chemically reacting water tunnel experiment. It is argued that the axial vortex pair in the flow arises from the plume momentum normal to the free stream, the momentum flux being equivalent to the impulse from the buoyant force.

DOI: 10.1103/PhysRevFluids.5.094701

I. INTRODUCTION

The structure, trajectory, and mixing rate of transverse jets have been investigated in numerous experiments, such as in Refs. [1–5]. The jets are driven by the initial momentum flux from the nozzle, without buoyancy differences between the jet fluid and the ambient fluid. A prominent feature of the flow is a pair of counter-rotating vortices. In the far field, those vortices are nearly parallel and move with the free stream. Broadwell and Breidenthal [6] argue that a temporal, two-dimensional vortex pair can model the dynamics and mixing, resulting from a line impulse. Above the mixing transition, the mixing is entrainment limited, so that the simple dilution model discussed in Ref. [6] describes the mixing rate, to within an adjustable constant.

It appears that the buoyancy-driven plume has been less studied [7–10]. In contrast to the jet, the conserved quantity for such a plume is the buoyancy force rather than the jet thrust. Morton *et al.* [9] presented an analysis of a source of buoyancy and Morton [10] extended this to allow for mass, momentum, and buoyancy. As described in detail in the sections to follow, Morton [10] determined the location of the mixing transition for a plume without cross-flow and considered the case of momentum being in the vertical direction and of the same sign as the buoyancy forces. Other studies such as those by Hofer and Hutter [11] and Schatzmazz [12], presented numerical schemes for evaluating forced and angled plumes with a given set of initial conditions. Lane-Serff and Baines [13] proposed a mathematical model that clearly presented a division of vertical plumes into three basic categories: buoyant jets, mass sources, and pure plumes. The main focus of their work was, however, concentrated on studies of angled plumes. The mathematical model presented by Lane-Serff and Baines is found to be valid only for cases with buoyancy and momentum flux with the same sign.

II. ANALYSIS

The present work is a direct extension of an analysis developed for the transverse jet by Broadwell and Breidenthal [6] to transverse plumes. It is a dimensional argument based on fundamental

[*]Present address: Department of Aerospace Engineering, University of Illinois at Urbana-Champaign, Urbana, Illinois 61801, USA; pranjan2@illinois.edu
[†]Also at Pacific Wildland Fire Sciences Laboratory, USA Forest Service, Seattle, Washington 98103, USA.
[‡]breident@aa.washington.edu

physics. For example, consider as the simplest case the canonical turbulent jet into a quiescent fluid. At any far-field station x, the characteristic width of the jet is independent of both nozzle diameter and the kinematic viscosity. The conserved quantity in the flow is the integrated momentum flux from the nozzle thrust, so that the nozzle diameter has no effect on the far-field jet, except through the nozzle thrust. If the Reynolds number is much larger than 1, viscous forces associated with the largest eddies are small compared to their inertial forces. Since entrainment is dominated by the largest eddies, the growth is independent of Reynolds number. It follows that the width of the jet can only depend on x since it is the only length scale available.

The appropriate temporal problem for the spatially developing transverse jet is the line, or two-dimensional (2D), vortex pair [6]. In a Lagrangian sense, the nozzle thrust on the primary flow in the spatial problem is a momentary, external impulse in the 2D temporal problem. For the transverse plume, the temporal problem is the two-dimensional thermal. The external buoyant force per unit length is continuous and constant, rather than from a momentary impulse that subsequently vanishes. The only difference in the analysis of the transverse jet and the transverse plume is the duration of the external force. The temporal problem should be a valid approximation of the corresponding spatial problem if the curvature of the spatial flow can be ignored. This approximation is expected to be asymptotically valid in the far field of the flow, where the curvature asymptotically vanishes. The conserved quantity is the buoyant force per unit length and per unit mass,

$$B = \frac{\text{const} \times g_0' V_n A_0}{V_\infty} = \frac{\text{length}^3}{\text{time}^2}, \tag{1}$$

where g' is the buoyancy acceleration. The subscript 0 indicates the initial value at the nozzle. The nozzle velocity is V_n, the nozzle area is A_0, and the free-stream velocity is V_∞. From dimensional considerations,

$$\tilde{\delta}(t) = \text{const} \times B^{1/3} t^{2/3}, \tag{2}$$

where $\tilde{\delta}(t)$ is the vortex size as a function of time t. The nozzle thrust and buoyant force act as external forces on the free stream. According to the vorticity equation, torque from the nonconservative forces generates vorticity [14].

For a self-similar transverse plume, any reasonable definition of the plume width is equally arbitrary and equally justified. This arbitrary scale is proportional to both the separation between the vortices and any reasonable definition of their diameter. Since the aspect ratio of the plume is of the order one, the vortex separation is of the same order of magnitude as any other reasonable definition of the vortex diameter or the plume width. In the current study, the vortex size $\tilde{\delta}(t)$ is defined as the visible width of the plume from the side view as observed during the experiment.

Assuming a Galilean transformation, the downstream station x is related to t by

$$x = V_\infty t, \tag{3}$$

and the spatial problem becomes

$$\frac{\delta(x)}{l} = \text{const} \times \left(\frac{x}{l}\right)^{2/3}, \tag{4}$$

where

$$l = \frac{B}{V_\infty^2} \tag{5}$$

is an intrinsic length scale of the spatial problem related to the radius of curvature near the origin.

Equation (4) for the transverse plume compares with

$$\frac{\delta}{l_j} = \text{const} \times \left(\frac{x}{l_j}\right)^{1/3} \tag{6}$$

for the transverse jet, where the corresponding length scale is

$$l_j = \left(\frac{T}{\rho V_\infty^2}\right), \tag{7}$$

according to Ref. [6]. Here, T is the jet thrust and ρ is the free-stream density.

III. MIXING AND FLAME LENGTH

In the current study, when a fluid consisting of an acid or alkaline solution rapidly reacts with the free stream, the rate of disappearance of the reacting fluid corresponds to the rate at which the two fluids react with one another. Considering a generic fuel combustion process, the length of the flame can be qualitatively described as the distance over which the reactant disappears or the reaction product is formed. Quantitatively, the flame length may correspond to the distance over which molecular mixing and entrainment with a stoichiometric amount of fluid takes place. In the current study, the flame length is described based on the early seminal work of Hottel [15] and is derived using Broadwell's dilution agreement in Ref. [6]. A key experiment by Weddell, reported in Ref. [15], describes the effect of discharging a water jet consisting of an alkaline solution with phenolphthalein as a pH indicator, into a stationary acidic reservoir. The jet fluid, upon reacting with a sulfuric acid solution, turns colorless as it entrains and mixes downstream from the nozzle. The volume equivalence ratio ϕ is defined as the ratio of the volume of ambient fluid required to react completely with a unit volume of the jet fluid. As defined by Wendell, the *flame length* is the distance over which the red color of the pH indicator completely disappears. Based on the mixing and reaction models by Ref. [6], the reaction process is initially characterized by large-scale entrainment of the acidic solution and is followed by an inviscid cascade to the Kolmogorov scale λ_0. The amount of time t_d required for a jet to entrain a given volume of ambient fluid and then the subsequent inertial cascade scales with the rotation period of the large-scale eddies. Since the Kolmogorov scale is

$$\lambda_0 \sim \left(\frac{\nu^3 d}{V_n}\right)^{1/4}, \tag{8}$$

the time required for the jet to diffuse over this distance is

$$t_\lambda \sim \left(\frac{\mathrm{Sc}}{\mathrm{Re}_d^{1/2}}\right)\frac{d}{V_n}, \tag{9}$$

where Sc is the Schmidt number and Re_d is the Reynolds number at the nozzle exit. For the transverse plume, the smallest Reynolds number in the flow field is at the nozzle. The ratio of the diffusion time to the large-scale breakdown time is expressed as

$$T \sim \frac{\mathrm{Sc}}{\mathrm{Re}_d^{1/2}}. \tag{10}$$

Hence, for sufficiently large Reynolds number, the diffusion time t_d is faster than the large-scale rotation period. Since the flame length is controlled by the entrainment and the cascade times, it is essentially independent of the Reynolds number above the mixing transition.

The flame length depends on the volume equivalence ratio ϕ. From Broadwell's dilution argument [6], per unit time, the volume of mixed fluid at the flame tip divided by the volume of the nozzle fluid must be proportional to $(\phi + 1)$. Hence,

$$\frac{V_\infty \delta_f^2}{V_n A_0} = \mathrm{const} \times (\phi + 1), \tag{11}$$

where δ_f is the width of the plume at the flame tip. Equation (11) suggests that with increases in free-stream velocity, the volume of the injected reactant per unit time is spread out over a longer length of the plume. Consequently, the width of the plume at the flame tip is reduced in order to maintain the same volume necessary to react all the injected fluid.

Equations (1)–(11) yield

$$\frac{x_f}{d} = \text{const} \times \left(\frac{V_n^2}{g_0' d}\right)^{1/2} \left(\frac{V_\infty}{V_n}\right)^{3/4} (\phi + 1)^{3/4}, \tag{12}$$

where x_f is the streamwise station at the flame tip and d is the nozzle diameter. The flame length depends weakly on the nozzle Richardson number,

$$\text{Ri}_0 = \frac{g_0' d}{V_n^2}. \tag{13}$$

We have implicitly assumed that the nozzle thrust is sufficiently small compared to the buoyant flux. This assumption is not true at the nozzle if Ri_0 is less than one. Farther from the nozzle, however, the accumulated impulse of a continuous buoyant force eventually surpasses that of the initial jet thrust, so that Eq. (12) should be asymptotically valid at a sufficiently large equivalence ratio. Morton [10] determined the location of this transition for a plume without cross-flow.

With a cross-flow, the transition between a momentum-dominated flow and a buoyancy-dominated flow can be estimated by equating the impulse per unit length of the jet with the plume in their corresponding temporal problems.

They are equal at time

$$t^* = \frac{T/\rho}{BV_\infty}, \tag{14}$$

corresponding to station

$$x^* = \frac{T/\rho}{B}. \tag{15}$$

This can be expressed as

$$x^* = \frac{\rho_0}{\rho} \frac{V_\infty V_n}{g_0'}, \tag{16}$$

where ρ_0 is the density of the injected fluid. Equation (13) is expected to be valid if $x^* \ll x_f$.

IV. EXPERIMENT

An aqueous plume was introduced through the test-section ceiling of a water tunnel, which provided the cross-flow. The water tunnel apparatus is described in Eroglu *et al.* [16]. Briefly, the test section is 0.7 m high, spans 0.7 m, and is 3 m long, through which a dilute and transparent solution of sulfuric acid flowed. A red solution of sodium hydroxide, sodium chloride, and phenolphthalein (a *p*H indicator) drained into the water tunnel through a jet nozzle of 0.019 m diameter from a reservoir above the water tunnel. The solution drained exclusively under gravitational flow, with no other momentum source. When two fluids mixed, a rapid chemical reaction caused the red injected solution to disappear. The volume equivalence ratio (the volume ratio to ambient to inject fluid required to effect dilution and disappearance) was varied by changing the relative concentrations of the acid and base. The velocity of the jet was estimated from the measured volume flow rate as determined by the rate at which the liquid emptied from the reservoir. No correction was made to the velocity profile for the thickness of the nozzle boundary layers. Figure 1 illustrates the schematics for the evolving flow geometry and Fig. 2 represents the experiment layout used in the current study.

The nozzle Reynolds number Re_0 varied between 400 and 6000. While this range is not always above the Reynolds number of the mixing transition, approximately a few thousand, the important requirement for the flame length is that the mixing be entrainment limited by the flame tip. So the

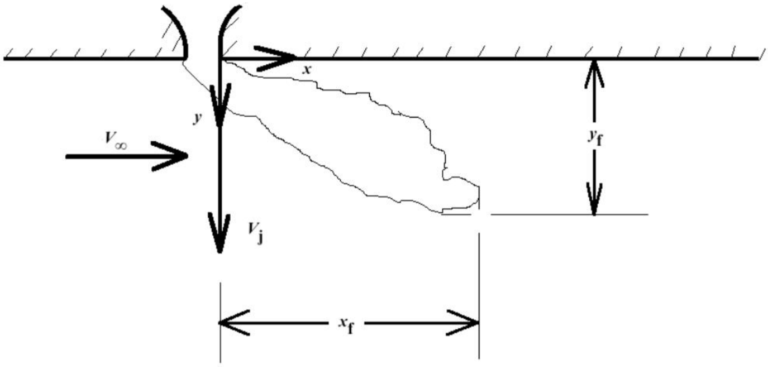

FIG. 1. Flow geometry.

Reynolds number at the flame tip must be sufficiently large. From Eqs. (2)–(13), it is

$$\mathrm{Re}_f = \left(\frac{g_0' V_n A_0}{V_\infty}\right)^{2/3} \left(\frac{x_f}{V_\infty}\right)^{1/3} \frac{1}{\nu}, \tag{17}$$

where ν is the kinematic viscosity of the fluid. The Reynolds number at the flame tip varied from 1000 to 21 000.

The coordinates at the tip of the red plume were measured using a video recording from a 6.1-megapixel camera with 3× optimal zoom (35 mm equivalent: 36–108 mm) which permitted taking pictures with an equivalent shutter speed of 1/1400 s, providing an appropriate resolution of the flame tip. The nozzle fluid was nearly saturated with salt in order to minimize the fraction of the total flame length that was influenced by initial nozzle momentum rather than buoyancy. While holding the nozzle speed constant, the tunnel speed was progressively varied from run to run. The velocity ratio of the free stream to nozzle flows ranged from 0.6 to 22. The chord flame length is defined in terms of the flame tip coordinates,

$$c_f \equiv \left(x_f^2 + y_f^2\right)^{1/2}. \tag{18}$$

The chord flame length normalized by the nozzle diameter is plotted as a function of the velocity ratio for different values of volume equivalence ratio in Fig. 3. The streamwise flame length normalized by the nozzle diameter is shown in Fig. 4.

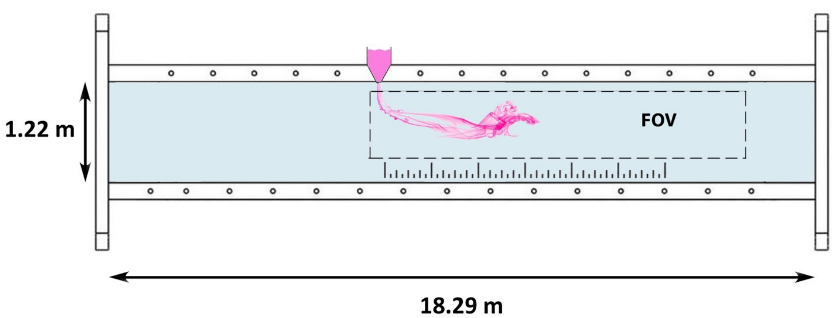

FIG. 2. Flow geometry.

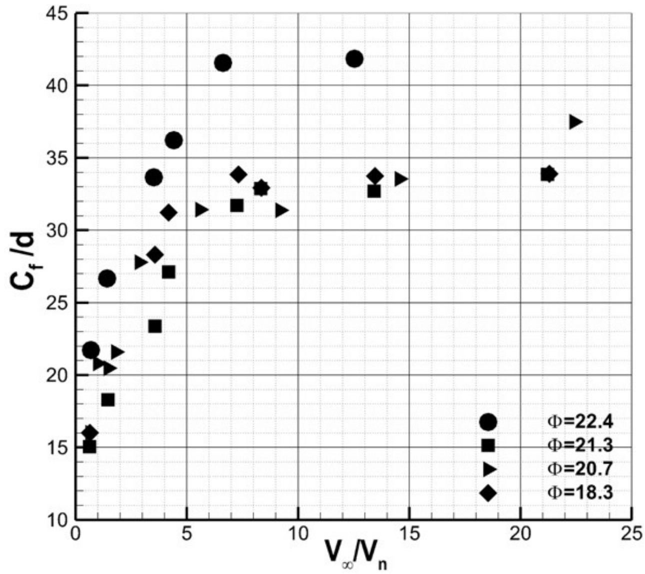

FIG. 3. Flame chord length for varying equivalence ratio.

From Eq. (12), the model suggests a different normalization, defined by

$$X_f = \frac{x_f}{d\left(\frac{V_n}{g_0' d}\right)^{1/2}\left(\frac{V_\infty}{V_n}\right)^{3/4}(\phi+1)^{3/4}}. \tag{19}$$

This normalized flame length is shown in Fig. 5. As observed, the data appear to collapse along the analytical solution for large values of $\frac{V_\infty}{V_n}$, suggesting the model reasonably describes the transverse plume even when the plume is near the wall. Evidently, the nearby wall does not affect

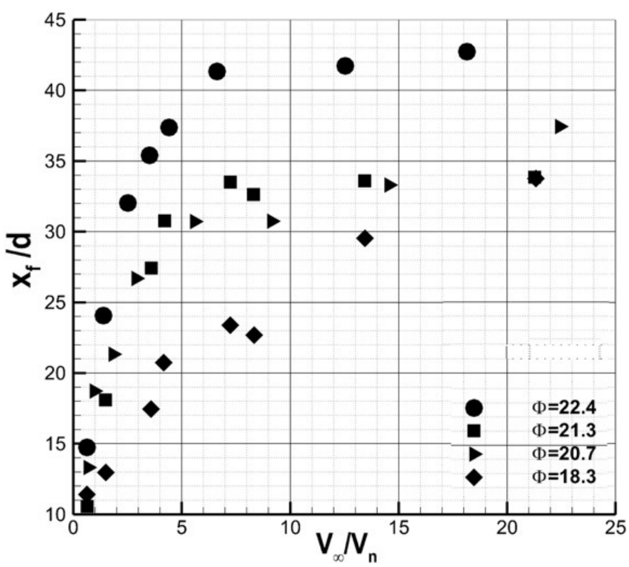

FIG. 4. Downstream flame length for different ϕ.

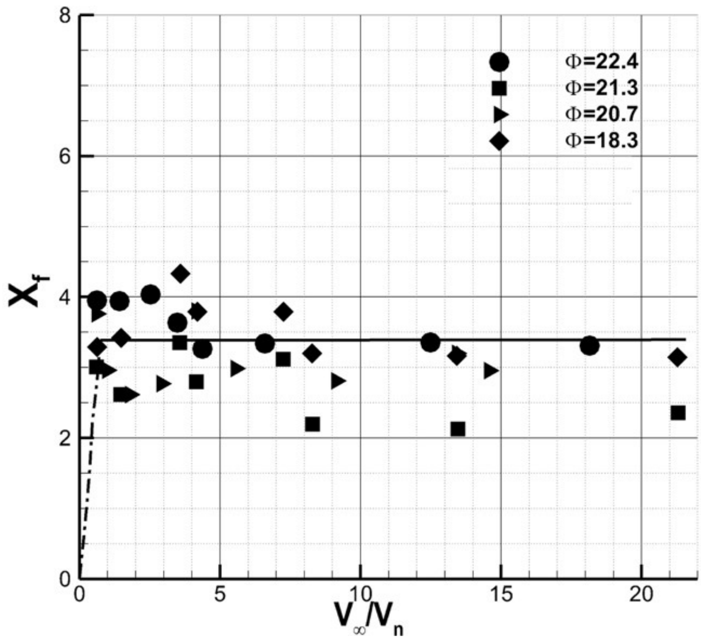

FIG. 5. Normalized downstream flame length.

the entrainment much, at least over this range of velocity ratios. The authors argue that the physics depends on the dimensionless measure of buoyant effects, the Richardson number as well as the Reynolds number, since the molecular mixing is strongly affected by mixing transition. Necessary values of both Ri and Re are achieved even for low values of the velocity ratios in Figs. 3–5. According to the Galilean transformation within this model, the only effect of V_∞ is to transport the buoyant plume more rapidly downstream. The plume Reynolds number is based on the size and vertical velocity component of the plume, independent of V_∞.

V. DISCUSSION

As with the transverse jet, the flame length of the transverse plume is independent of the Reynolds number Re_0 (for fixed) above a certain critical value. All data shown are from this regime. For lower Reynolds numbers, the flame length is much longer in an aqueous flow. This behavior, typical of mixing in turbulent flows, is due to the sensitivity of the mixing rate to the presence of small-scale turbulent motions. The critical value for this mixing transition is of the order of a thousand. According to Eq. (12), the model predicts that the streamwise flame length x_f/d should vanish in the limit of $V_\infty/V_n \to 0$. Furthermore, the flame length goes as $(\phi + 1)$ raised to the power $3/4$. However, it is clear that the chord flame length c_f/d cannot vanish in that limit. Furthermore, similarity requires that the flame length be proportional to $(\phi + 1)$ there. Experiments by Rouse *et al.* [17], Papanicolaou and List [18], Shabbir and George [19], and others all show that the buoyant fluid must travel a specific distance from its source in order to entrain and to mix sufficient ambient fluid to dilute the source fluid to a specified concentration. As a consequence, the chord flame length at any equivalence ratio is finite for $V_\infty/V_n = 0$. It is clear that two different regimes exist, with a transition between them at some $V_\infty/V_n > 0$ where the chord flame length is a minimum.

From Fig. 5, the velocity ratio for minimum chord flame length is evidently less than about 0.6. This is consistent with the value of about 0.6 observed in the transverse jet of Ref [6]. Such a minimum is expected to correspond in both flows to the formation of a pair of counter-rotating vortices.

FIG. 6. Flow visualization of the Fric and Roshko vortices.

VI. APPLICATION TO WILDFIRES

This study was originally motivated by questions related to the wild land fire behavior. Among other things, wild land fire behavior includes the intensity (energy release rate) of the fire, rate of spread, and the variability of these properties over time. An intense, fast moving fire with a highly variable rate or direction of spread is dangerous for firefighters and more difficult to bring under control. Any insight into the properties likely to produce particularly dangerous fire behavior has the potential to save lives, as well as thousands of dollars.

When applied to a wild land fire, it is first important to distinguish what is meant by flame length. The term *flame* as used previously in this paper refers to the visible mixing portion of the buoyant outflow. To scale up a wild land fire, this flame is much larger than the combustion zone, and more comparable to a large portion of the smoke plume. For clarity, *flame* will still be used.

In the wild land fire context, the minimum flame length mentioned previously corresponds to the maximum mixing rate, which would presumably lead to the most intense fire behavior. The integrated buoyancy flux over the fire area

$$F \equiv \frac{g\dot{E}}{\rho c_p \Theta}, \tag{20}$$

where $\dot{E}$ is the rate of energy release and is the absolute temperature of the incident wind. Consider an idealized wildfire propagating downwind along an advancing front. A simple dimensional argument suggests that the most intense fire would occur for a critical wind speed,

$$V_{\infty_{\text{crit}}} \cong F^{1/3} D^{-1/3} = \left(\frac{g\dot{E}}{\rho c_p \Theta D} \right)^{1/3}, \tag{21}$$

where D is some measure of the transverse width of the fire. For the heat content of the fuel h (J kg^{-1}), the fuel density w (kg m^{-2}), and the fire's downwind advancement speed r (m s^{-1}), this can be written as

$$V_{\infty_{\text{crit}}} = \left(\frac{ghwr}{\rho c_p \Theta} \right)^{1/3}, \tag{22}$$

Because the water tunnel design approximates a *point source* fire, it is most relevant to a fire where the transverse and longitudinal extents are comparable, or small. As an example application of this, consider the 2003 Canberra fire in Australia. The estimated fuel load and rate of spread for this fire are 2.5 kg m^{-2} and 1.3 m s^{-1}, respectively. The heat content of forest fuels is approximately

17 MJ kg^{-1}. Using these fire properties with approximate values for g, ρ, c_p, and Θ (9.8 m s^{-2}, 1.1 kg m^{-3}, 1004 J kg^{-1} k^{-1}, and 300 K, respectively) then yields a critical wind speed of 12 m s^{-1}. This suggests that Eq. (22) provides reasonable wind speed values, given real values for the input parameters.

The normalized flame length of a real fire would be slightly different from that in the water tunnel. In the water tunnel, all of the buoyancy is introduced at the nozzle. In a real fire, on the other hand, buoyancy is continuously added from the origin to the flame tip. Another flow feature that may threaten firefighters is Fric and Roshko lee vortices [20], shown in Fig. 6. While these tornadolike vortices seem to have little effect on the far-field flame length of the plume, they may play a critical role on some wild land fires by first lofting and then propagating burning embers downwind, as noted by Cunningham *et al.* [21]. Firebrands sometimes overrun and defeat fire breaks constructed by firefighters, igniting new fires downwind of old ones.

VII. CONCLUDING REMARKS

The analysis and the comparison of the results with observation have concentrated on the far-field behavior of transverse plumes. From the conservation of buoyant force, the growth law of the corresponding temporal flow has been derived. A simple dilution argument then predicts the flame length of the spatial flow. The measured flame length of the transverse plume is in accord with this description of the far-field behavior. Notably, there is a minimum in the predicted flame length at an intermediate velocity ratio. This suggests the approximate conditions for the most intense wildfires.

---

[1] J. Keffer and W. Baines, The round turbulent jet in a cross-wind, J. Fluid Mech. **15**, 481 (1962).

[2] Y. Kamotani and I. Greber, Experiments on a turbulent jet in a cross flow, AIAA J. **10**, 1425 (1972).

[3] S. Smith and M. Mungal, Mixing, structure and scaling of the jet in cross flow, J. Fluid Mech. **357**, 83 (1998).

[4] L. Cortelezzi and A. Karagozian, On the formation of the counter-rotating vortex pair in transverse jets, J. Fluid Mech. **446**, 347 (2001).

[5] A. Karagozian, Transverse jets and their control, Prog. Energy Combust. Sci. **36**, 531 (2010).

[6] J. Broadwell and R. Breidenthal, Structure and mixing of a transverse jet in incompressible flow, J. Fluid Mech. **148**, 405 (1984).

[7] J. Middleton, The rise of forced plumes in a stably stratified cross flow, Boundary Layer Meteorol. **36**, 187 (1986).

[8] M. Golay, Numerical modeling of buoyant plumes in a turbulent, stratified atmosphere, Atmos. Environ. **16**, 2373 (1982).

[9] B. R. Morton, G. I. Taylor, and J. Turner, Turbulent gravitational convection from maintained and instantaneous sources, Proc. R. Soc. A **234**, 1 (1956).

[10] B. Morton, Forced plumes, J. Fluid Mech. **5**, 151 (1959).

[11] K. Hofer and K. Hutter, Turbulent jet diffusion in stratified quiescent ambients, part I: Theory, J. Non-Equilib. Thermodyn. **6**, 31 (1981).

[12] M. Schatzmann, The integral equations for round buoyant jets in stratified flows, J. Appl. Math. Phys. **29**, 608 (1978).

[13] G. Lane-Serff and P. Baines, Eddy formation by dense flows on a slope in a rotating fluid, J. Fluid Mech. **363**, 229 (1998).

[14] P. Saffman, *Vortex Dynamics* (Cambridge University Press, Cambridge, U.K., 1992).

[15] H. Hottel, Burning in laminar and turbulent fuel jets, *in Proceedings of the 4th Symposium (International) on Combustion* (Elsevier, Amsterdam, 1953), Vol. 4, pp. 97–113.

[16] A. Eroglu and R. E. Breidenthal, Exponentially accelerating jet in cross flow, AIAA J. **36**, 1002 (1998).
[17] H. Rouse, C. S. Yih, and H. W. Humphreys, Gravitational convection from a boundary source, Tellus **4**, 201 (1952).
[18] P. Papanicolaou and E. List, Statistical and spectral properties of tracer concentration in round buoyant jets, Int. J. Heat Mass Transfer **30**, 2059 (1987).
[19] A. Shabbir and W. George, Experiments on a round turbulent buoyant plume, J. Fluid Mech. **275**, 1 (1994).
[20] T. Fric and A. Roshko, The vortical structure in the wake of a transverse jet, J. Fluid Mech. **279**, 1 (1994).
[21] P. Cunningham, S. L. Goodrick, M. Y. Hussaini, and R. R. Linn, Coherent vortical structures in numerical simulations of buoyant plumes from wildland fires, Int. J. Wildland Fire **14**, 61 (2005).